IEEE Access
Multidisciplinary | Rapid Review | Open Access Journal

Received October 9, 2019, accepted October 17, 2019, date of publication October 24, 2019, date of current version November 20, 2019.

Digital Object Identifier 10.1109/ACCESS.2019.2949301

Analysis on Eddy Current Losses in Stator Windings of Large Hydro-Generator Considering Transposed Structure Based on Analytical Calculation Method

XU BIAN AND YANPING LIANG
College of Electrical and Electronic Engineering, Harbin University of Science and Technology, Harbin 150080, China
Corresponding author: Yanping Liang (liangyanping2010@126.com)

This work was supported in part by the National Natural Science Foundation of China under Grant 51807040, in part by the Natural Science Foundation of Heilongjiang Province under Grant QC2018065, and in part by the Fundamental Research Foundation for Universities of Heilongjiang Province under Grant 2018JC025.

ABSTRACT Aimed at the problem that the existing calculation method of eddy current losses in stator windings of large hydro-generators cannot consider the transposed structure and circulating current, the equivalent circuit model considering the actual transposed structure and circulating current is established, and the analytical calculation method for eddy current losses of stator winding is proposed in this paper, which is suitable for different transposed structures. Then, eddy current losses of stator transposed winding in an 180MW hydro-generator is analyzed by the proposed method and validated by the finite element method. Finally, the influence of the transposed structure on eddy current losses of stator windings is analyzed quantitatively and compared with the existing calculation method. The results show that the value and distribution trend of eddy current losses in strands change a lot when considering the influence of circulating current and the actual transposed structure, and the influence is different for different transposed structures, which must be considered.

INDEX TERMS Analytical calculation method, eddy current losses, large hydro-generator, stator winding, transposed structure.

I. INTRODUCTION

The accurate calculation of additional losses in stator windings of the large hydro-generator plays an important role in the design of stator windings and is also the prerequisite for the subsequent temperature calculation [1], [2]. Additional losses in stator windings of the large hydro-generator mainly consist of circulating current losses generated by circulating current between strands in one stator bar and eddy current losses generated by eddy current in one strand of the stator bar, which are all caused by the leakage magnetic field. In order to reduce circulating current losses, the transposed structure is adopted by parallel strands in slot portion [3], and then every transposed strand changes its position in stator slot along the axial direction of generator, leading to the leakage magnetic flux linked by one transposed strand is different along the axial direction, which will affect the distribution of eddy current and eddy current losses in every transposed strand. Moreover, the circulating current cannot be eliminated completely by the transposed structure [4], and the distribution of eddy current losses is also influenced by the circulating current [5], [6]. Therefore, the actual transposed structure and circulating current should be considered when calculating eddy current losses in stator windings of large hydro-generators.

There are mainly three kinds of calculation methods for eddy current losses in copper conductors, including analytical formula method, equivalent circuit method and finite element method. The influence of eddy current is considered by the litz-wire resistance in [7], [8] and the analytical formula for resistance considering skin and proximity effects is derived. However, the leakage magnetic flux linked by litz-wires is very different from that linked by stator windings in large hydro-generators. Therefore, the analytical formula cannot be used in the calculation of eddy current losses in stator windings. Eddy current losses in stator windings induced by

The associate editor coordinating the review of this manuscript and approving it for publication was Xiaodong Sun.

the slot leakage magnetic flux of traction motors, small power induction motors and large converter-fed hydropower generators are obtained in [9]–[11] by analytical formulas, which cannot consider the actual transposed structure. In equivalent circuit method, every conductor is divided into many sub-conductors according to the flow path of the eddy current, and then eddy current losses can be obtained by solving the equivalent circuit consisting of sub-conductors. A wideband lumped circuit model of eddy current losses in a coaxially insulated coil is presented in [12]. The equivalent circuit of transformer winding is established in [13]–[15] to calculate eddy current losses of windings in transformer considering the skin effect. The equivalent circuit method is widely used in losses analysis [16], [17], but little is used in windings of large hydro-generators. In finite element method, eddy current losses of every conductor can be obtained by establishing the finite element model. The eddy current of circular current-carrying conductors considering skin effect and nonlinear permeability is obtained in [18] and eddy current losses of litz wire considering different bundle structures and pitch lengths is obtained in [19] by two-dimensional finite element method. Eddy current losses of stator windings in high speed permanent magnet AC motors and switched reluctance machines are obtained in [20]–[22] by two-dimensional finite element method. Though the three-dimensional finite element model for the calculation of circulating current losses in stator windings considering the actual transposed structure is established in [23], [24], however eddy currents in stator strands are not considered. The computational accuracy of eddy current losses depends on the layer number of subdivision elements, and that of every transposed strand should be divided into many layers along the changing direction of magnetic field. Then, a huge number of subdivision elements will be generated due to the great disparity of sizes between strand gauge and strand length and the three-dimensional finite element model is hard to solve.

In the existing method for eddy current losses in stator windings of large hydro-generators, it is assumed that circulating currents between stator strands in a stator bar are ignored and the distribution of leakage magnetic field along the axial direction is the same in the stator slot, thus eddy current losses can be obtained by solving the leakage magnetic field in a two-dimensional stator slot section [25] and the transposed structure and circulating current are not considered. Aimed at that problem, the equivalent circuit model considering actual transposed structure and circulating current is established, and the analytical calculation method for eddy current losses of stator windings with different transposed structures is proposed in this paper. Eddy current loss of stator windings in an 180MW hydro-generator is calculated by the proposed analytical calculation method and validated by the multi-section two-dimensional finite element method. The influence of the transposed structure on the eddy current loss of stator windings is analyzed and compared with the existing calculation method.

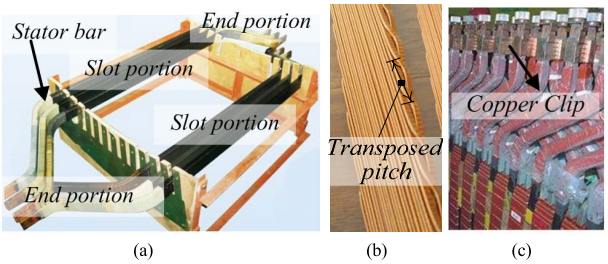

FIGURE 1. The structure of stator windings in large hydro-generators. (a) The structure of the stator bar. (b) The transposed structure in the slot portion of stator bars. (c) The connection structure in the end portion of stator bars.

II. ANALYTICAL CALCULATION METHOD OF THE EDDY CURRENT LOSS IN STATOR TRANSPOSED WINDINGS

The stator winding of large hydro-generators consists of many stator bars, which is shown in Fig.1(a). The stator bar is made of many rectangle cross-sectional solid strands in parallel, and the transposed structure is used in the slot portion of the stator bar, which is shown in Fig.1(b). All transposed strands are connected together in the end portion of one stator bar and connected to the next stator bar by the copper clip, which is shown in Fig.1(c).

A. CALCULATION PRINCIPLE

The eddy current exists in every stator strand, which is generated by the difference of the leakage magnetic flux in different position of one stator strand. For large hydro-generators, there are many poles, leading to the small span for the end portion of the stator bar, thus the contribution of the leakage magnetic flux in end portion to the eddy current in every stator strand is very small. Therefore, the eddy current in every stator strand is almost generated by the leakage magnetic flux in slot portion.

The leakage magnetic flux is almost transversal distributed in slot portion, so the eddy current distribution in one strand is almost along the strand height direction. The single transposed strand is taken as an example, and the flow path of eddy current is shown in Fig.2(a). When considering the transposed structure, the slot leakage magnetic flux linked by one transposed strand is different along the axial direction, affecting the eddy current in one transposed strand, which should be simulated by complex three-dimensional model.

In order to simplify the solution procedure, the equivalent method of the eddy current in every transposed strand is presented. The schematic figure of the equivalent method is shown in Fig.2(b), in which the strand with 4 sub strands and 3 transposed pitches are taken as examples. In the actual calculation, the number of sub conductors is determined by the calculation accuracy and the number of transposed pitch is determined by the transposed structure.

The transposed path of strand is considered as straight line in every transposed pitch. The distribution of slot leakage magnetic flux is considered uniform in one transposed pitch and is different between different transposed pitches because

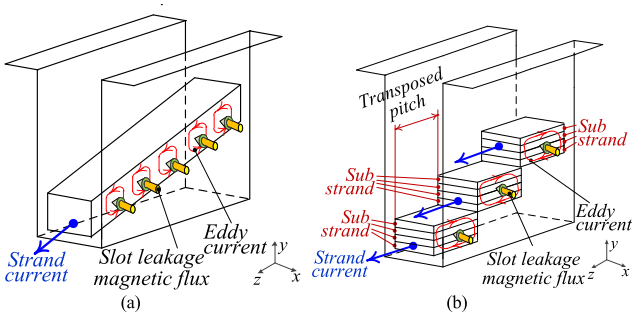

FIGURE 2. The eddy current in one stator transposed strand and its equivalent method. (a) The flow path of eddy current. (b) Equivalent method of the eddy current.

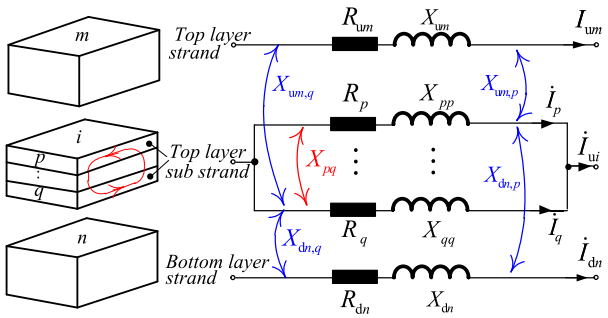

FIGURE 3. Equivalent circuit model of every stator transposed strand in every transposed pitch for calculating the eddy current loss.

of the transposed structure. In every transposed pitch, every strand is divided into many sub strands along the strand height direction. The eddy current losses can be obtained by calculating the current of sub strands in every transposed pitch.

B. EQUIVALENT CIRCUIT MODEL

The source of the eddy current is the difference of the slot leakage magnetic flux linked by different sub strands in one stator transposed strand. The slot leakage magnetic flux is represented by the slot leakage reactance, the equivalent circuit model of every transposed strand in every transposed pitch for calculating the eddy current loss can be established, which is shown as Fig.3.

For the convenience of illustration, taking the top layer #i strand as an example, the equivalent circuit model in Figure 3 only includes the top layer #i strand, the top layer #m strand and the bottom layer #n strand. If there are N_1 strands in the top layer bar, N_2 strands in the bottom layer bar and N sub strands in #i strand, $R_p(p = 1 \cdots N)$ represent the resistance of #p sub strand in one transposed pitch, $X_{pq}(p, q = 1 \cdots N)$ represent the mutual leakage reactance between #p sub strand and #q sub strand in one transposed pitch, $X_{\mathrm{u}m,p}(p = 1 \cdots N, m = 1 \cdots N_1)$ represent the mutual leakage reactance between the top layer #m strand and #p sub strand in one transposed pitch, $X_{\mathrm{d}n,p}(p = 1 \cdots N, n = 1 \cdots N_2)$ represent the mutual leakage reactance between the bottom layer #n strand and #p sub strand in one transposed pitch, $\dot{I}_p(p = 1 \cdots N)$ represent the current of #p sub strand in one transposed pitch, $\dot{I}_{\mathrm{u}m}(m = 1 \cdots N_1)$ represent the current of the top layer #m strand, $\dot{I}_{\mathrm{d}n}(n = 1 \cdots N_2)$ represent the current of the bottom layer #n strand.

C. CALCULATION METHOD OF EDDY CURRENT LOSS

According to the equivalent circuit model, the equivalent circuit equation of every transposed strand in every transposed pitch can be established as (1).

$$\begin{cases} (\boldsymbol{R} + \mathrm{j}\boldsymbol{X})\,\dot{\boldsymbol{I}} + \mathrm{j}\,[\boldsymbol{X}_{\mathrm{u}} \;\; \boldsymbol{X}_{\mathrm{d}}] \begin{bmatrix} \dot{\boldsymbol{I}}_{\mathrm{u}} \\ \dot{\boldsymbol{I}}_{\mathrm{d}} \end{bmatrix} = \boldsymbol{0} \\ [11 \cdots 1]\,\dot{\boldsymbol{I}} = \dot{I}_{\mathrm{u}i} \end{cases} \tag{1}$$

where $\boldsymbol{R}$ represent the resistance matrix of sub strands, $\boldsymbol{X}$ represent the reactance matrix of sub strands, $\boldsymbol{X}_{\mathrm{u}}$ represent the reactance matrix between sub strands and the top layer strand, $\boldsymbol{X}_{\mathrm{d}}$ represent the reactance matrix between sub strands and the bottom layer strand, $\dot{\boldsymbol{I}}$ represent the current matrix of sub strands, $\dot{\boldsymbol{I}}_{\mathrm{u}}$ represent the current matrix of the top layer strands, $\dot{\boldsymbol{I}}_d$ represent the current matrix of the bottom layer strands, which are shown as (2)-(6).

$$\boldsymbol{R} = \begin{bmatrix} R_1 & -R_2 & 0 & \cdots & \cdots & 0 \\ 0 & R_2 & -R_3 & 0 & \cdots & 0 \\ \vdots & 0 & \ddots & \ddots & \ddots & \vdots \\ \vdots & \vdots & \ddots & \ddots & \ddots & 0 \\ 0 & 0 & \cdots & 0 & R_{(N-1)} & -R_N \end{bmatrix} \tag{2}$$

$$\boldsymbol{X} = \begin{bmatrix} X_{11} - X_{21} & X_{12} - X_{22} & \cdots & X_{1N} - X_{2N} \\ X_{21} - X_{31} & X_{22} - X_{32} & \cdots & X_{2N} - X_{3N} \\ \vdots & \vdots & \ddots & \vdots \\ X_{(N-1)1} - X_{N1} & X_{(N-1)2} - X_{N2} & \cdots & X_{(N-1)N} - X_{NN} \end{bmatrix} \tag{3}$$

$$\boldsymbol{X}_u = \begin{bmatrix} X_{\mathrm{u}1,1} - X_{\mathrm{u}1,2} & X_{\mathrm{u}2,1} - X_{\mathrm{u}2,2} & \cdots & X_{\mathrm{u}N_1,1} - X_{\mathrm{u}N_1,2} \\ X_{\mathrm{u}1,2} - X_{\mathrm{u}1,3} & X_{\mathrm{u}2,2} - X_{\mathrm{u}2,3} & \cdots & X_{\mathrm{u}N_1,2} - X_{\mathrm{u}N_1,3} \\ \vdots & \vdots & \ddots & \vdots \\ X_{\mathrm{u}1,(N-1)} - X_{\mathrm{u}1,N} & X_{\mathrm{u}2,(N-1)} - X_{\mathrm{u}2,N} & \cdots & X_{\mathrm{u}N_1,(N-1)} - X_{\mathrm{u}N_1,N} \end{bmatrix} \tag{4}$$

where $X_{\mathrm{u}i,p} = 0(p = 1 \cdots N)$ (5)-(6), as shown at the bottom of the next page.

In (1), $\dot{\boldsymbol{I}}$ is unknown matrix, other matrixes are known matrixes. $\dot{I}_{\mathrm{u}m}$ and $\dot{I}_{\mathrm{d}n}$ can be obtained by [26], in which circulating current between strands is considered.

The resistance R_p can be obtained by (7).

$$R_p = \rho \frac{l}{S} \tag{7}$$

where ρ represent the resistivity of the sub strand, l represent the length of the transposed pitch, S represent the area of the sub strand.

The reactance X_{pq} can be obtained by (8). The reactance $X_{\mathrm{u}m,p}$ and $X_{\mathrm{d}n,p}$ can be obtained by the

TABLE 1. Basic parameters of the 180-MW hydrogenerator.

Parameter	Value	Parameter	Value
Rated current(A)	7331.4	Rated frequency(Hz)	50
Number of pole	72	Number of stator slots	594
Number of strands in one stator bar	50	Number of parallel branches	2
Height of strand(mm)	2	Width of strand(mm)	8

same method.

$$X_{pq} = \frac{\omega \mu_0 l}{b_s} \min(h_p, h_q) \tag{8}$$

where ω represent the angular frequency, μ_0 represent the permeability of vacuum, b_s represent the width of the stator slot, h_p represent the distance between #p sub strand and the slot opening, h_q represent the distance between #q sub strand and the slot opening.

The eddy current loss of #i strand in #α transposed pitch can be obtained by (9).

$$P_{i\alpha} = \sum_{p=1}^{N} |\dot{I}_p|^2 R_p - |\dot{I}_{ui}|^2 \frac{R_p}{N} \tag{9}$$

Then, the eddy current loss of #i strand can be obtained by (10).

$$P_i = \sum_{\alpha=1}^{N_s} P_{i\alpha} \tag{10}$$

where N_s represent the number of transposed pitch.

III. RESULTS OF EDDY CURRENT LOSSES CONSIDERING TRANSPOSED STRUCTURE AND VALIDATION

A. RESULTS OF EDDY CURRENT LOSSES

The stator transposed bar of a 180-MW hydro-generator is taken as an example in this paper, the basic parameters of which are shown in Table 1. The material of the strand is copper.

The incomplete transposed structure is adopted in the slot portion of the stator bar, the transposed path of which is shown in Fig.4. In every transposed pitch, all strands in one stator bar move the height of one strand according to the transposed direction and the corresponding transposed angle

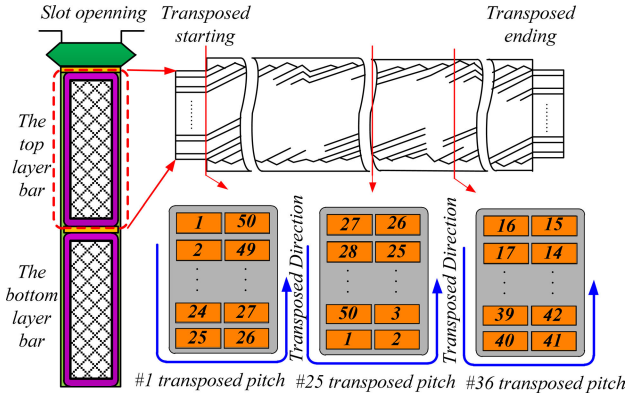

FIGURE 4. The transposed pitch number and strand number of the stator bar in the 180-MW hydro-generator.

is 7.2°. The transposed angles of the stator bar in the top and bottom layer are both 345.6°, and then the transposed strands are divided into 48 transposed pitches and numbered #1 to #48 from the transposed starting to the transposed ending.

The top layer #27 strand and #48 strand are taken as examples to show the equivalent transposed path obtained by the analytical calculation method, the actual and equivalent transposed path is shown in Fig.5.

The transposed angle of the stator bar is 345.6°, that is to say, every strand is two transposed pitches short to occupy all positions of strands in one stator bar. In every transposed pitch, the actual transposed path of strand is slash, which is equivalent to straight line. Every strand is divided into 16 sub strands and numbered #1 to #16 from the slot opening to the slot bottom.

The mutual-leakage reactance between 16 sub strands of the top layer #1 strand in #1 transposed pitch is shown in Fig.6(a). The mutual-leakage reactance between 16 sub strands of the top layer #1 strand and the bottom layer strands in #1 transposed pitch is shown in Fig.6(b), the value of which is the same as the self-leakage reactance of 16 sub strands of the top layer #1 strand. The mutual-leakage reactance between 16 sub strands of the top layer #1 strand and other top layer strands is the same as Fig.6(b).

The current RMS and current phase of the top and bottom layer strands is calculated by the method in [21], which is shown in Fig.7. The current RMS and current phase are different for different strands because of the circulating current

$$\boldsymbol{X}_d = \begin{bmatrix} X_{d1,1} - X_{d1,2} & X_{d2,1} - X_{d2,2} & \cdots & X_{dN_2,1} - X_{dN_2,2} \\ X_{d1,2} - X_{d1,3} & X_{d2,2} - X_{d2,3} & \cdots & X_{dN_2,2} - X_{dN_2,3} \\ \vdots & \vdots & \ddots & \vdots \\ X_{d1,(N-1)} - X_{d1,N} & X_{d2,(N-1)} - X_{d2,N} & \cdots & X_{dN_2,(N-1)} - X_{dN_2,N} \end{bmatrix} \tag{5}$$

$$\dot{\boldsymbol{I}} = \begin{bmatrix} \dot{I}_1 \\ \dot{I}_2 \\ \vdots \\ \dot{I}_N \end{bmatrix}, \quad \dot{\boldsymbol{I}}_u = \begin{bmatrix} \dot{I}_{u1} \\ \dot{I}_{u2} \\ \vdots \\ \dot{I}_{uN_1} \end{bmatrix}, \dot{\boldsymbol{I}}_d = \begin{bmatrix} \dot{I}_{d1} \\ \dot{I}_{d2} \\ \vdots \\ \dot{I}_{dN_2} \end{bmatrix} \tag{6}$$

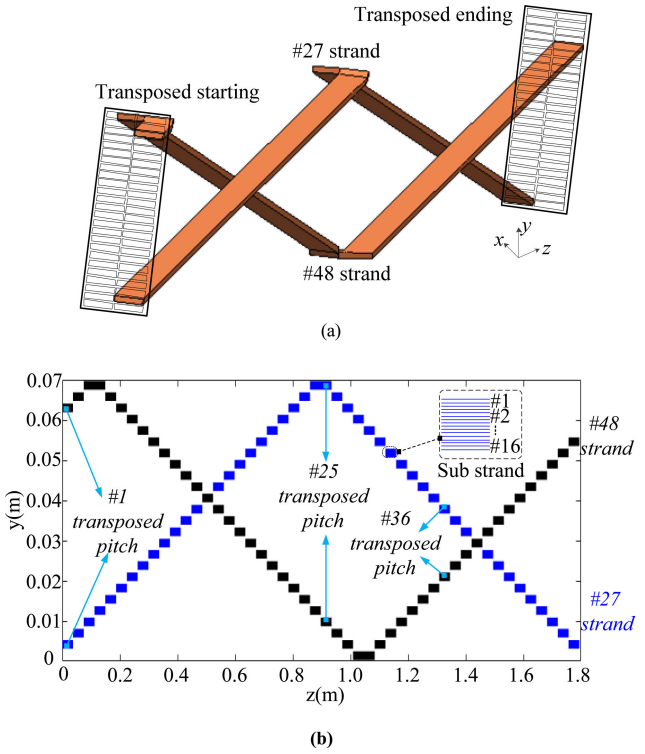

FIGURE 5. The equivalent transposed path of the top layer #27 strand and #48 strand obtained by the analytical calculation method when the transposed angle is 345.6°. (a) The actual transposed path. (b) The equivalent transposed path.

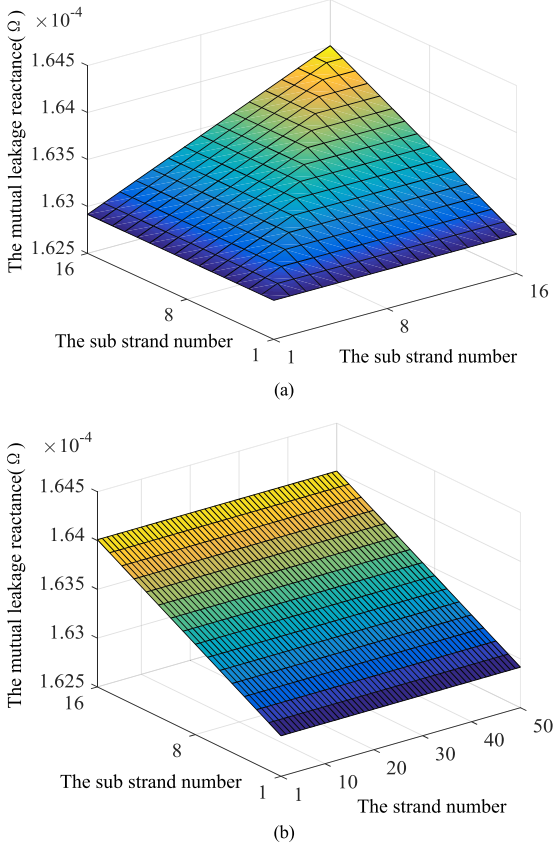

FIGURE 6. The leakage reactance of the top layer #1 strand in #1 transposed pitch. (a) The mutual leakage reactance between sub strands. (b) The mutual leakage reactance between sub strands and the bottom layer strands.

between different strands in the same stator bar. The current RMS of #27 strand is the largest and that of #48 strand is the smallest in the top layer, the current RMS of #27 strand is the largest and that of #45 strand is the smallest in the bottom layer. The circulating current is generated by both slot and end leakage magnetic flux. When the transposed angle is 345.6°, the offset effect of the slot leakage magnetic flux on the end leakage magnetic flux is the strongest and circulating current is the smallest, and the contribution of the end leakage magnetic flux to circulating current is more prominent than the slot leakage magnetic flux. The end portion length of the top and bottom layer bar is different, leading to the end leakage magnetic flux linked by the top and bottom layer bar is different, therefore, where the minimum value appears is different.

The current density of sub strands in the top layer #27 strand, #48 strand, the bottom layer #27 strand and #45 strand in #1, #25 and #36 transposed pitch are shown in Fig.8. The current density distribution of sub strands is different in different transposed pitches for the same strand, the eddy current in one strand decreases from the slot opening to the bottom because the value of slot leakage magnetic flux density almost decreases from the slot opening to the bottom. In one transposed pitch, the current density distribution of sub strands in different strands is different. We can observe by comparing Fig.8(b) and Fig.8(c) that in #1 transposed pitch, the current density maximum of sub strands in the top layer #48 strand is larger than that in the bottom layer #25 strand though the current RMS of the bottom layer #25 strand is larger, because in #1 transposed pitch, the value of slot leakage magnetic flux density where the top layer #48 strand locates is larger. Therefore, the current density maximum of sub strands in one strand is not only related to the current value of a strand, but also related to the value of slot leakage magnetic flux density where the strand locates.

The eddy current losses of the top and bottom layer strands obtained by the analytical calculation method when the number of sub strands is 4, 8, 12, 16 and 20 are shown in Fig.9. The distribution of eddy current losses in the top layer strands is different from the bottom layer strands though the same transposed structure is adopted by the top and bottom layer strands. The value of eddy current losses in the top layer strands is much larger than the bottom layer strands because the slot leakage magnetic flux density of the top layer strands is much larger than the bottom layer strands. With the increase of the number of sub strands, the eddy current losses of the top and bottom layer strands will increase when the number of sub strands is less than 16 and that are almost not changed when the number of sub strands is more than 16. Therefore, the strand is divided into 16 sub strands.

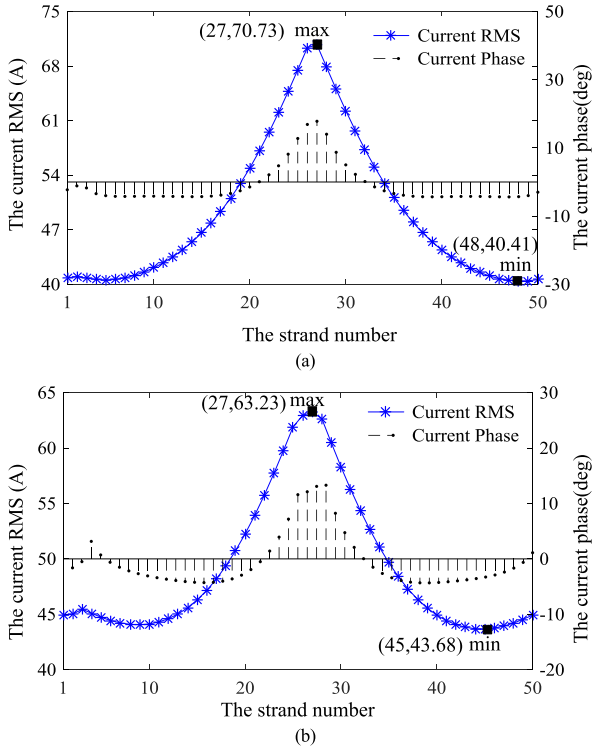

FIGURE 7. The current RMS and current phase of the top and bottom layer strands considering circulating current when the transposed angle is 345.6°. (a) The top layer strands. (b) The bottom layer strands.

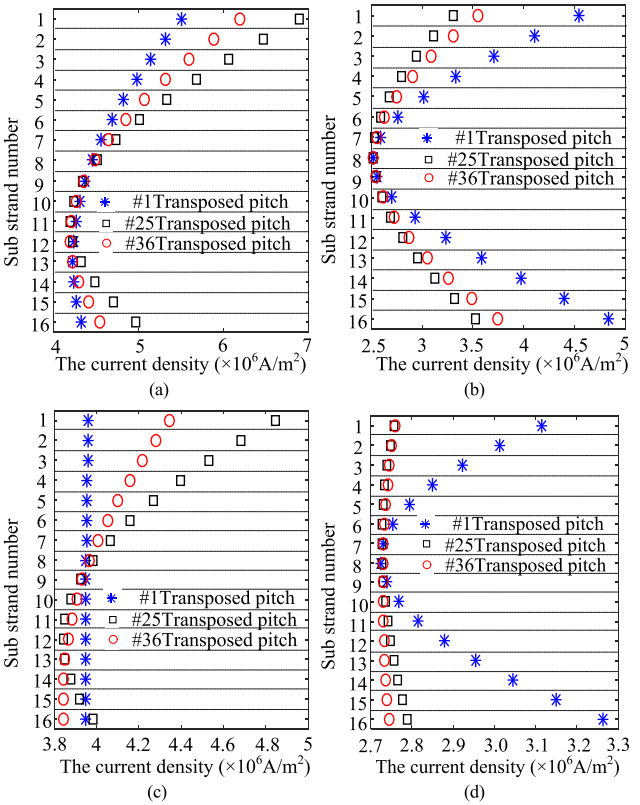

FIGURE 8. The current density of sub strands in different transposed pitches. (a) The top layer #27 strand. (b) The top layer #48 strand. (c) The bottom layer #27 strand. (d) The bottom layer #45 strand.

B. VALIDATION OF ANALYTICAL CALCULATION METHOD

The multi-section two-dimensional finite element method is used to validate the analytical calculation method, the solution model of which is shown in Fig.10(a) and the circuit connection is shown in Fig.10(b).

The number of sections is 48 and numbered $S1$ to $S48$ from the transposed starting to the transposed ending, which is the same as the analytical calculation method. In every section, the solution region consists of the strand region and the air region. The strand region is considered as eddy-current region and the air region is considered as non-eddy-current region. In the circuit, the strands of different sections with the same number are connected into one branch and the current of strands are the same as Fig.7.

The two-dimensional eddy current field is used to solve the solution region. The boundary value problem of the two-dimensional linear eddy current field expressed by the z component of the vector magnetic potential $\dot{A}_z$ is shown as follows.

$$\begin{cases} \dfrac{1}{\mu_0}\left(\dfrac{\partial^2 \dot{A}_z}{\partial x^2}+\dfrac{\partial^2 \dot{A}_z}{\partial y^2}\right) = -\dot{J}_s + j\omega\sigma\dot{A}_z \\ \left.\dfrac{\partial \dot{A}_z}{\partial n}\right|_{\overline{ghabcd}} = \left.\dfrac{\partial \dot{A}_z}{\partial n}\right|_{\overline{fe}} = 0 \\ \left.\dot{A}_z\right|_{\overline{fg}} = \left.\dot{A}_z\right|_{\overline{ed}} = 0 \end{cases} \tag{11}$$

where $\dot{J}_s$ represent the source current density, σ represent the conductivity, n represent the normal direction of boundaries.

The current density distribution of strands in $S1$, $S25$ and $S36$ section calculated by multi-section two-dimensional finite element method is shown in Fig.11. The current density distribution of strands in different sections is different due to the transposed structure. The current density value and distribution of the top layer #27 strand, #48 strand, the bottom layer #27 strand, #45 strand is the same as Fig. 8.

Eddy current losses of the top and bottom layer strands in #1, #25 and #36 transposed pitch calculated by analytical calculation method and multi-section two-dimensional finite element method are compared in Fig.12. Eddy current losses of strands in different transposed pitches are different because of different distribution of current and different strand position in stator slot. The calculation results obtained by analytical calculation method are near that obtained by finite element method, and the maximum relative error is less than 3%.

IV. INFLUENCE OF TRANSPOSED STRUCTURE ON EDDY CURRENT LOSSES IN STATOR WINDINGS

In order to analyze the influence of transposed structure on eddy current losses in stator windings, eddy current losses

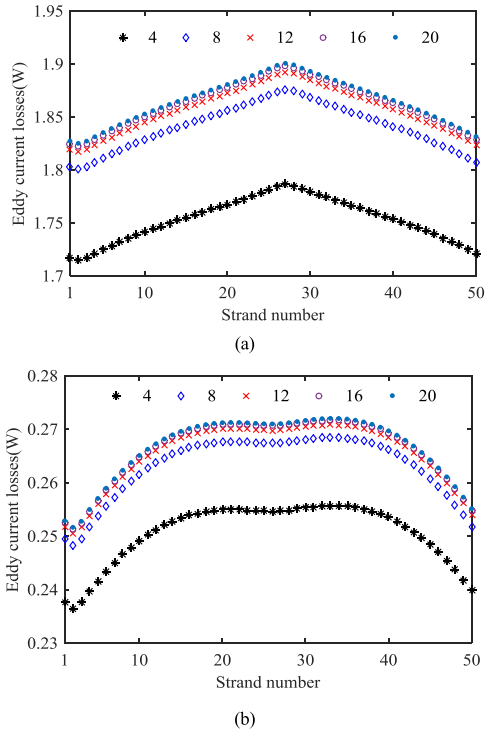

FIGURE 9. The eddy current losses of the top and bottom layer strands when the number of sub strands is different. (a) The top layer strands. (b) The bottom layer strands.

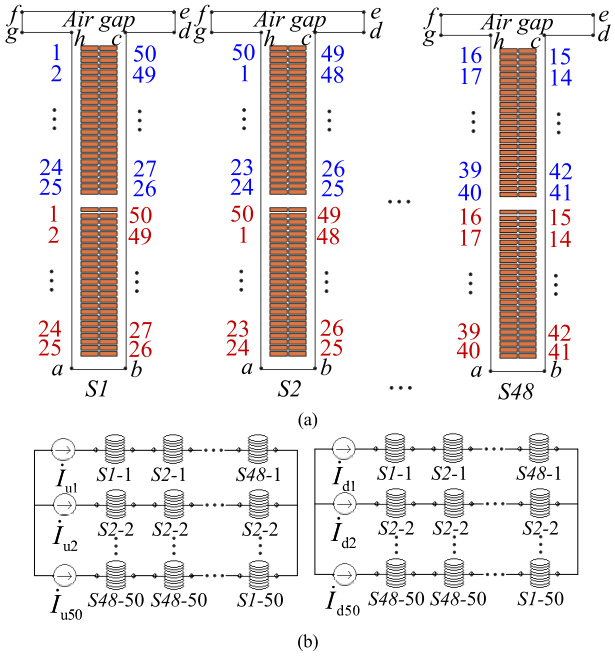

FIGURE 10. The calculation model of multi-section two-dimensional finite element method. (a) Solution region. (b) Circuit connection.

of stator transposed strands in the 180-MW hydro-generator is calculated by the proposed analytical calculation method when the transposed angle of the top and bottom layer bar are both 288°. The transposed strands are divided into 40 transposed pitches, and the equivalent transposed path of the top layer #27 strand and #48 strand is shown in Fig.13.

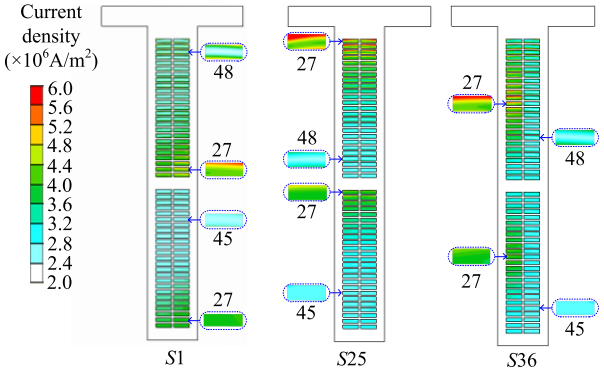

FIGURE 11. The current density distribution of strands in different sections calculated by multi-section two-dimensional finite element method.

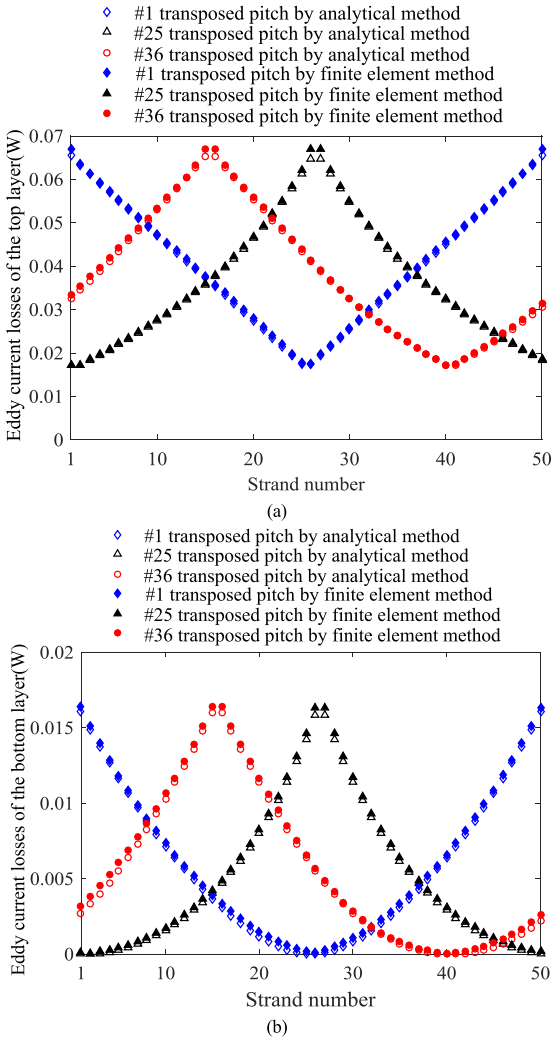

FIGURE 12. Eddy current losses of strands in different transposed pitch calculated by analytical calculation method and multi-section two-dimensional finite element method. (a) The top layer strands. (b) The bottom layer strands.

The current RMS and current phase of the top and bottom layer strands when the transposed angle is 288° is shown in Fig.14, which is different from Fig.7 because of the different transposed angle. When the transposed angle is 288°,

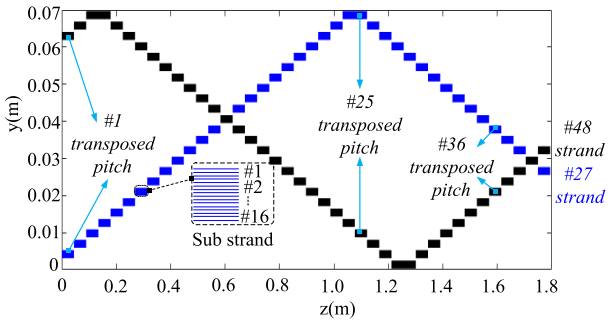

FIGURE 13. The equivalent transposed path of the top layer #27 strand and #48 strand obtained by the analytical calculation method when the transposed angle is 288°.

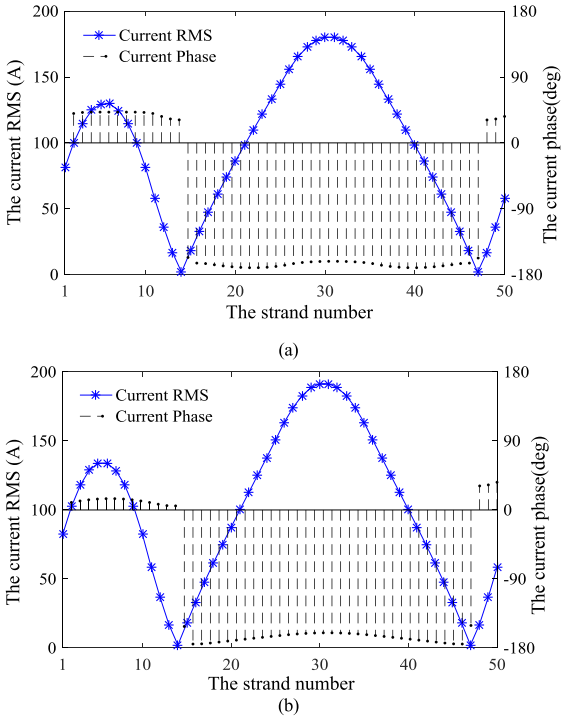

FIGURE 14. The current RMS and current phase of strands considering circulating current when the transposed angle is 288°. (a) The top layer strands. (b) The bottom layer strands.

the spare slot leakage magnetic flux besides that offset the end leakage magnetic flux will also generate circulating current. Therefore, the current RMS and phase difference is larger than that when the transposed angle is 345.6°.

Eddy current losses of the top and bottom layer strands in #1, #25 and #36 transposed pitch calculated by analytical calculation method when the transposed angle is 288° are shown in Fig.15. Though the strand position in #1, #25 and #36 transposed pitch is the same as that when the transposed angle is 345.6°, eddy current losses of strands are very different because of the different distribution of strand current, which directly affects the distribution of slot magnetic flux density. Therefore, the distribution of strand current has a great effect on the eddy current losses in strands.

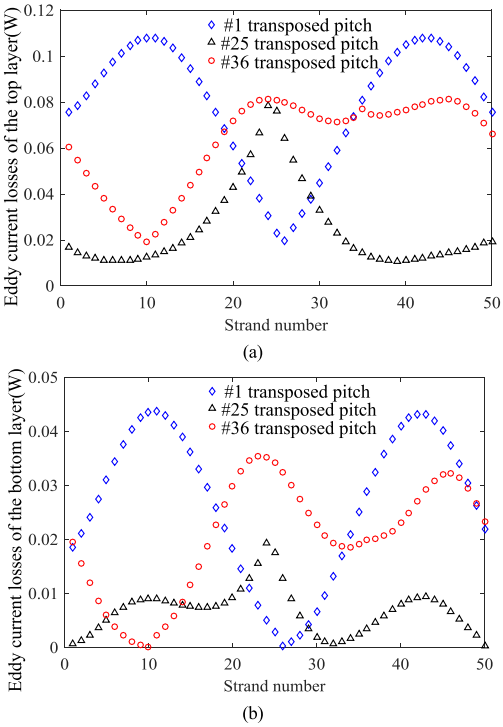

FIGURE 15. Eddy current losses of strands in different transposed pitch calculated by analytical calculation method when the transposed angle is 288°. (a) The top layer strands. (b) The bottom layer strands.

Eddy current losses of the top and bottom layer strands obtained by the analytical calculation method when the transposed angle is 288° are shown in Fig.16, which are different from Fig.9.

The strand number with the largest eddy current loss will change when different transposed structures are adopted because of the different distribution of the slot leakage magnetic field and different transposed structure. The strand with large current in Fig. 14 doesn't have large eddy current losses in Fig. 16, because eddy current losses are related to the slot leakage magnetic flux linked by different sub strands in one strand. Though the current of one strand is large, the value of slot leakage magnetic flux density where that strand locates is small, and then the eddy current losses of that strand will be small.

In order to compare with the existing calculation method, eddy current losses of the top and bottom layer strands in the 180-MW hydro-generator are calculated by the existing calculation method, in which the current of every strand in one stator bar is considered the same and the transposed structure is ignored, thus two-dimensional finite element method is usually used. The calculation result obtained by the existing calculation method is shown in Fig. 17 no matter which transposed structure is adopted. We can observe by comparing Fig. 17, Fig. 9 and Fig. 16 that the value and distribution trend of eddy current losses in strands change a lot when considering the influence of circulating current and the actual transposed structure, and the influence is different for different transposed structures.

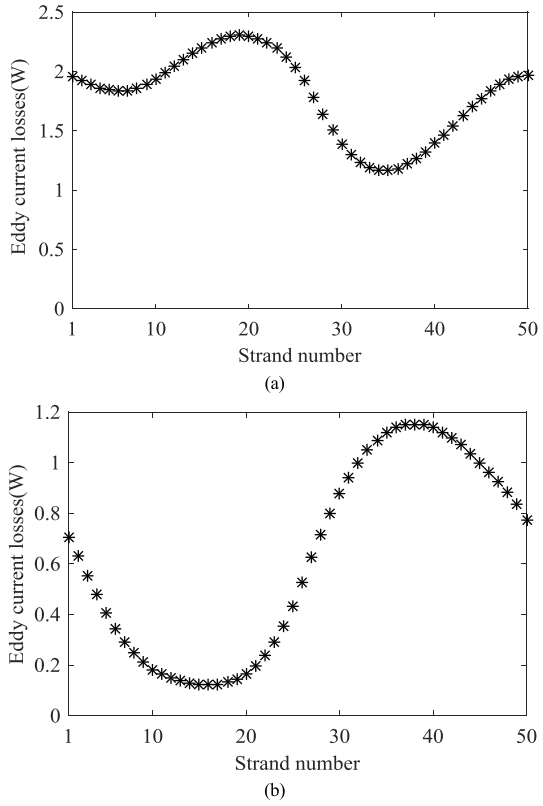

FIGURE 16. Eddy current losses of the top and bottom layer strands when the transposed angle is 288°. (a) The top layer strands. (b) The bottom layer strands.

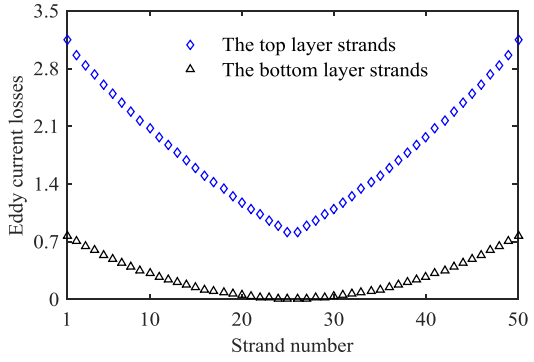

FIGURE 17. Eddy current losses of the top and bottom layer strands by the existing calculation method.

V. COUCLUSION

A fast analytical calculation method for eddy current losses of stator windings considering actual transposed structure and the non-uniform distribution of strand current due to circulating current is proposed and validated by the finite element method. In the proposed method, the number of sub strands has a great effect on the calculation results. With the increase of the number of sub strands, eddy current losses of strands will increase. For the 180-MW hydro-generator analyzed in this paper, 16 sub strands can meet the calculation accuracy.

The leakage magnetic flux is almost transversal distributed in slot portion, so the eddy current distribution in every strand is almost along the strand height direction, leading that the current density varies at different heights of every strand. The current density distribution of the same strand is different for different transposed pitches. In one transposed pitch, the current density distribution of different strands is different. The current density maximum of every strand is not only related to the current value of strand, but also related to the value of slot magnetic flux density where the strand locates.

The eddy current losses in strands is not related to a strand current directly, but is related to the value of slot leakage magnetic flux density where the strand locates, which is determined by the current distribution of all strands and the position of all strands in stator slot. The value and distribution trend of eddy current losses in strands change a lot when considering the influence of circulating current and the actual transposed structure, and the influence is different for different transposed structures, which must be considered when calculating eddy current losses in stator transposed windings.

REFERENCES

[1] R. Wrobel, A. Mlot, and P. H. Mellor, "Contribution of end-winding proximity losses to temperature variation in electromagnetic devices," *IEEE Trans. Ind. Electron.*, vol. 59, no. 2, pp. 848–857, Feb. 2012, doi: 10.1109/TIE.2011.2148686.

[2] G.-H. Zhou, L. Han, Z.-N. Fan, H.-B. Zhang, X.-C. Dong, J. Wang, Z. Sun, and B.-D. Zhang, "Ventilation cooling design for a novel 350-MW air-cooled turbo generator," *IEEE Access*, vol. 6, pp. 62184–62192, 2018, doi: 10.1109/ACCESS.2018.2875757.

[3] C. Wang, Y. Liang, L. Ni, D. Wang, and X. Bian, "Calculation and analysis of the strands short-circuit in stator transposition bar for large generators," *IEEE Access*, vol. 7, pp. 36132–36139, 2019, doi: 10.1109/ACCESS.2019.2905362.

[4] M. Fujita, Y. Kabata, T. Tokumasu, K. Nagakura, M. Kakiuchi, and S. Nagano, "Circulating currents in stator coils of large turbine generators and loss reduction," *IEEE Trans. Ind. Appl.*, vol. 45, no. 2, pp. 685–693, Mar/Apr. 2009, doi: 10.1109/TIA.2009.2013572.

[5] T. Asada, Y. Baba, N. Nagaoka, A. Ametani, J. Mahseredjian, and K. Yamamoto, "A study on basic characteristics of the proximity effect on conductors," *IEEE Trans. Power Del.*, vol. 32, no. 4, pp. 1790–1799, Aug. 2017, doi: 10.1109/tpwrd.2016.2590962.

[6] C. Di, I. Petrov, and J. J. Pyrhönen, "Design of a high-speed solid-rotor induction machine with an asymmetric winding and suppression of the current unbalance by special coil arrangements," *IEEE Access*, vol. 7, pp. 83175–83186, 2019, doi: 10.1109/ACCESS.2019.2925131.

[7] I. Lope, J. Acero, and C. Carretero, "Analysis and optimization of the efficiency of induction heating applications with Litz-wire planar and solenoidal coils," *IEEE Trans. Power Electron.*, vol. 31, no. 7, pp. 5089–5101, Jul. 2016, doi: 10.1109/TPEL.2015.2478075.

[8] Q. Deng, J. Liu, D. Czarkowski, M. K. Kazimierczuk, M. Bojarski, H. Zhou, and W. Hu, "Frequency-dependent resistance of Litz-wire square solenoid coils and quality factor optimization for wireless power transfer," *IEEE Trans. Ind. Electron.*, vol. 63, no. 5, pp. 2825–2837, May 2016, doi: 10.1109/tie.2016.2518126.

[9] J. D. Widmer, R. Martin, and B. C. Mecrow, "Precompressed and stranded aluminum motor windings for traction motors," *IEEE Trans. Ind. Appl.*, vol. 52, no. 3, pp. 2215–2223, May/Jun. 2016, doi: 10.1109/tia.2016.2528226.

[10] M. Dems and K. Komeza, "The influence of electrical sheet on the core losses at no-load and full-load of small power induction motors," *IEEE Trans. Ind. Electron.*, vol. 64, no. 3, pp. 2433–2442, Mar. 2017, doi: 10.1109/tie.2016.2587817.

[11] E. L. Engevik, M. Valavi, and A. Nysveen, "Analysis of additional eddy-current copper losses in large converter-fed hydropower generators," in *Proc. ICEM*, Sep. 2018, pp. 1067–1073, doi: 10.1109/ICELMACH.2018.8506810.

[12] P. Holmberg, M. Leijon, and T. Wass, "A wideband lumped circuit model of eddy current losses in a coil with a coaxial insulation system and a stranded conductor," *IEEE Trans. Power Del.*, vol. 18, no. 1, pp. 50–60, Jan. 2003, doi: 10.1109/tpwrd.2002.803753.
[13] K. Preis, O. Biro, H. Reisinger, K. Papp, and I. Ticar, "Eddy current losses in large air coils with layered stranded conductors," *IEEE Trans. Magn.*, vol. 44, no. 6, pp. 1318–1321, June Jun. 2008, doi: 10.1109/tmag.2007.915829.
[14] M. Eslamian and B. Vahidi, "New equivalent circuit of transformer winding for the calculation of resonance transients considering frequency-dependent losses," *IEEE Trans. Power Del.*, vol. 30, no. 4, pp. 1743–1751, Aug. 2015, doi: 10.1109/tpwrd.2014.2361761.
[15] H. Zhang, S. Wang, D. Yuan, and X. Tao, "Double-ladder circuit model of transformer winding for frequency response analysis considering frequency-dependent losses," *IEEE Trans. Magn.*, vol. 51, no. 11, Nov. 2015. Art. no. 8402304, doi: 10.1109/TMAG.2015.2442831.
[16] X. Sun, Y. Shen, S. Wang, G. Lei, Z. Yang, and S. Han, "Core losses analysis of a novel 16/10 segmented rotor switched reluctance BSG motor for HEVs using nonlinear lumped parameter equivalent circuit model," *IEEE/ASME Trans. Mechatronics*, vol. 23, no. 2, pp. 747–757, Apr. 2018, doi: 10.1109/tmech.2018.2803148.
[17] X. Sun, K. Diao, G. Lei, Y. Guo, and J. Zhu, "Real-time HIL emulation for a segmented-rotor switched reluctance motor using a new magnetic equivalent circuit," *IEEE Trans. Power Electron.*, to be published, doi: 10.1109/TPEL.2019.2933664.
[18] M. P. Perkins, M. M. Ong, C. G. Brown, Jr., and R. D. Speer, "Analysis of conductor impedances accounting for skin effect and nonlinear permeability," in *Proc. IEEE Pulsed Power Conf.*, Jun. 2011, pp. 420–425, doi: 10.1109/ppc.2011.6191457.
[19] A. Roßkopf, E. Bär, C. Joffe, and C. Bonse, "Calculation of power losses in litz wire systems by coupling FEM and PEEC method," *IEEE Trans. Power Electron.*, vol. 31, no. 9, pp. 6442–6449, Sep. 2016, doi: 10.1109/TPEL.2015.2499793.
[20] M. Popescu and D. G. Dorrell, "Proximity losses in the windings of high speed brushless permanent magnet AC motors with single tooth windings and parallel paths," *IEEE Trans. Magn.*, vol. 49, no. 7, pp. 3913–3916, Jul. 2013, doi: 10.1109/TMAG.2013.2247382.
[21] D. A, Gonzalez and D. M. Saban, "Study of the copper losses in a high-speed permanent-magnet machine with form-wound windings," *IEEE Trans. Ind. Electron.*, vol. 61, no. 6, pp. 3038–3045, Jun. 2014, doi: 10.1109/tie.2013.2262759.
[22] M. Al Eit, F. Bouillault, C. Marchand, and G. Krebs, "2-D reduced model for eddy currents calculation in Litz wire and its application for switched reluctance machine," *IEEE Trans. Magn.*, vol. 52, no. 3, Mar. 2016, Art. no. 7401304, doi: 10.1109/tmag.2015.2486838.
[23] Y. Liang, X. Bian, L. Yang, and L. Wu, "Numerical calculation of circulating current losses in stator transposition bar of large hydro-generator," *IET Sci. Meas. Technol.*, vol. 9, no. 4, pp. 485–491, Jul. 2015, doi: 10.1049/iet-smt.2014.0230.
[24] Y. Liang, L. Wu, X. Bian, and H. Yu, "The influence of transposition angle on 3-D global domain magnetic field of stator bar in water-cooled turbo-generator," *IEEE Trans. Magn.*, vol. 51, no. 11, Nov. 2015, Art. no. 8113804, doi: 10.1109/tmag.2015.2450932.
[25] Y. D. Fan, X. S. Wen, H. M. Wang, and J. H. Seo, "Research on stator temperature field of a hydro-generator with skin effect," *IET Electr. Power Appl.*, vol. 5, no. 4, pp. 371–376, Apr. 2011, doi: 10.1049/iet-epa.2010.0185.
[26] X. Bian and Y. Liang, "Circuit network model of stator transposition bar in large generators and calculation of circulating current," *IEEE Trans. Ind. Electron.*, vol. 62, no. 3, pp. 1392–1399, Mar. 2015, doi: 10.1109/tie.2014.2347264.

XU BIAN was born in Harbin, China, in 1988. She received the B.S., M.S., and Ph.D. degrees in electrical machine from the Harbin University of Science and Technology, Harbin, China, in 2010, 2013, and 2016, respectively.

She is currently an Associate Professor with the Harbin University of Science and Technology. Her research interests include electromagnetic, fluid and thermal analysis, and design on electrical machines.

YANPING LIANG was born in Harbin, China, in 1963. She received the M.S. degree in electrical machine from the Harbin University of Science and Technology, Harbin, China, in 1988, and the Ph.D. degree in electrical machines from the Harbin Institute of Technology, Harbin, in 2005.

She is currently a Professor with the Harbin University of Science and Technology. Her research interests include electrical machine electromagnetic theory and design, large generator electromechanical energy conversion, and electromagnetic field calculation.

Dr. Liang is also a Senior Member of the China Electrotechnical Society.